RESEARCH ARTICLE   **OPEN ACCESS**

Investigation of influence of the indium doping on the properties of the Ga$_{(1-x)}$InxSb (x=0.10, 0.15, 0.25) crystals: the detached growth by the VDS-process

D. B. Gadkari*

*Freelance Research & Consultant: Crystal Growth and Technology
Embee-10A, Saibaba Nagar, Borivali (W), Mumbai-400092 India

ABSTRACT
A novel vertical directional solidification (VDS) process was utilized for the growth of III-V detached crystals and the study was focused to grow the indium doped Ga$_{(1-x)}$InxSb (x=0.10, 0.15, 0.25) bulk crystals. The influence of the Indium doping on the structural, electrical, optoelectronics, transport properties and band gap is investigated. The crystals exhibited their detachment by reduction in the resistivity to $1.1 \times 10^{-3} \Omega$.cm, conversion from p-type the perfect GaSb crystal to n-type the ternary Ga$_{(1-x)}$InxSb crystal and higher hole mobility 1.24×10^3cm^2/V.sec than the experimental value of mobility of binary GaSb crystal 1.12×10^3cm$_2$/V.sec. The electron mobility 2507cm^2/V.sec at 300K and 4037cm^2/V.sec at 77K were confirmed by the low temperature study. The band gap of the three Ga(1-x)InxSb ingots are tuned as -- i) 0.31 to 0.61eV, ii) 0.27 to 0.48eV, and iii) 0.27 to 0.33eV towards the band gap of the binary GaSb (0.68eV). XRD analysis of the grown crystals indicates that the III-V Sb based binary and ternary bulk crystals the preferred (022) growth direction. The stability and surface features of the entire detached ingots grown by VDS-process are close to the detached crystal growth in space.

Keywords **-** Directional solidification; .X-ray diffraction; Growth from melt, Antimonides; Semiconducting ternary compounds; Semiconducting III-V materials;

I. INTRODUCTION

III–V semiconductors crystals are prominent materials for the optoelectronics devices. The binary InSb and GaSb materials have the pseudo phase and highly miscible phase in the liquid-solid state of the Ga$_{(1-x)}$InxSb crystal growth. The physical, electronic and optical properties of the binary GaSb or InSb crystal vary continuously after doping of In or Ga respectively. The band gap and the lattice constant of the crystal can be tuned from 0.72 to 0.17 eV and 6.09 to 6.47 Å respectively by varying the 'x' component. These advantages have been applicable for the infrared detectors, semiconductor lasers, and in optoelectronic applications. Therefore a semiconductor compound with the higher carrier mobility and the tuneable band gap would be promising for the next-generation devices [1]; while, the III-V Nanowires (NWs) have been displayed the intriguing physical and chemical properties [2]. The mid-infrared (2-5µm) region has been beneficial for the ultrafast laser sources, the molecular spectroscopy, medical diagnostics and treatments [3]. Indium doped Ga$_{(1-x)}$InxSb crystal is precious for optoelectronic communications [4], moreover, NWs

are advantageous as photo-sensing elements for the broadband photo detectors [5]. The lattice constant modified by the indium (In) composition 'x' of the Ga(1-x)InxSb crystal changes the electrical properties, and the band gap [6]. The tuned band gap and electrical properties by the variation of 'x' in the Ga(1-x)InxSb crystal has been applied in the devices used for IR transmittance, and thermo-photovoltaic [7]. Though, a pseudo-binary InSb-GaSb phase grows in-homogeneously with increase in 'x', the segregation coefficient of 'In' at equilibrium is 0.2 [8]. The pseudo-binary GaSb-InSb phase of Ga(1-x)InxSb crystal and/or the highly miscible alloys (HMAs) in the liquid-solid state would be a hurdle and a challenge for crystal growth field [9]. The reason of inhomogeneous Ga(1-x)InxSb crystal growth is a segregated constitutional supercooling (CSC) due to the solute distribution at the interface [10]. A large thermal stress increases dislocation density and defects such as a twins, micro-cracks, inclusions and the solid-liquid interface shape does not remain flat /convex [11].

Advanced growth methods have been designed and fabricated to grow homogeneous and uniform crystals of the Ga(1-x)InxSb material by the

D. B. Gadkari*. International Journal of Engineering Research and Applications
www.ijera.com
ISSN: 2248-9622, Vol. 10, Issue 9, (Series-IV) September 2020, pp. 05-19

doping in the binary III-V Sb based crystals to restraint the In' segregation by decreasing dislocations and the native defects.

First growth methods: A new Bridgman growth process for the growth of Ga(1-x)InxSb crystal was operated to avoid crucible and crystal contact by the interface. The stability of capillary effect and the surface roughness were close to dewetted growth in space [12]. In addition to this, the InSb and GaSb dewetted crystals grown by the Bridgman were resulted in the highest Hall mobility and the electrical properties [13]. The etch pit density (EPD) was measured by international point counting method [14]. The influence of the temperature gradient and the growth velocity on Ga(1-x)InxSb crystal grown by the VB method, the axial and radial 'In' segregation was not suppressed [15]. GaSb crystal had a stable dewetting growth by an oxidising atmosphere, while the InSb crystal had not as the there was no wetting and thermodynamic stability. The self-stabilisation of the gas pressure was appeared [16]. The high quality Ga(1-x)InxSb crystal had been grown by using the sealed crucible in a vacuum lower than 1×10^{-4}pa [17]. The high-quality crystals of Ga(1-x)InxSb by 'In' doping in GaSb were grown by VB method and the crystals were converted from the p-type to n-type conductivity. The FWHM, and the dislocation density (1.275×10^3cm^{-2}) decreased, hence the crystalinity increased as the acceptors in GaSb substitute the 'In' element. Also, the mobility increased up to 2.512×10^3cm2/V.sec and the resistivity decreased to $0.521 \times 10^3 \Omega$.cm [18]. A horizontal travelling heater method (HTHM) had been applied to growth of the Ga(1-x)InxSb crystals to reduce the native defects ('Ga' vacancies). A uniform composition was achieved by horizontal Bridgman method (HBM). Ga(1-x)InxSb crystal grown by a conventional vertical Bridgman method (CHBM), where, the starting of the growth was sensitive to the source elements [19]. The lattice constant of Ga1-xInxSb changed by the 'In' or 'Al' element as an isoelectric dopant for 'Ga' and 'In' element, increased the carrier mobility in GaSb crystals with decrease in native defects by passivation-compensation [20]. When the CVBM was employed for the growth of Ga(1-x)InxSb:Te ingots by the stirred and non-stirred process; the segregation decreased by tellurium (Te), while no ingot cracks were observed for the stirred melt. The axial 'In' distribution increased lattice hardness and decreased the native defects by compen¬sation [21]. The construction of a furnace, in which the temperature is increasing with the height, minimizes the buoyancy convection. Detached growth (partial) was achieved for the gallium (Ga) doped InSb on earth, when, an ampoule coated with hexagonal boron nitride and oxide-free materials. Also the ampoule was filled with 20 kPa of Ar-10% H2 prior to sealing. Detached region of the ingot was lesser than the attached region [22].

Second growth methods: The rotating magnetic field (RMF): In a high-quality ingot of Ga0.86In0.14Sb grown by a RMF using VB method, the crystallinity improved by reducing the FWHM with the radial and axial segregation. In addition, the EPD (6.988×10^3cm^{-2}) decreased, the axial carrier mobility (1.618×10^3cm2/V.sec) increased, and the resistivity ($1.162 \times 10^{-3} \Omega$.cm) decreased [23]. Further increase in the RMF intensity increased the crystal's crystallinity and reduced a segregations and decreased a dislocation density (6.578×103cm−2), increased the mobility (1.738×103cm2/V sec), and reduced the resistivity ($1.149 \times 10−3 \Omega$ cm) [24]. RMF was also applied to grow Ga-doped 'Ge' by VGF method, decreased 'Ga' segregation and increased electrical properties [25]. An alternating magnetic field used to grow Ga1-xInxSb ingots by VB method, did not reduce the segregation [26]. A travelling heating method (THM) was applied RMF for the Ga1-xInxSb growth to shorten the crystal growth period, though, RMF changed a melt convection pattern [27].

Third growth method: III-V nanowires (NWs) have the huge potential for advanced applications due to the tuned band gap. Synthesis of large and high crystalline Ga(1-x)InxSb ($0.09 < x < 0.28$) (NWs) was a challenge. The stoichiometric uniform phase-purity crystalline NWs were grown by a chemical vapor deposition CVD). Ga0.91In0.09Sb NWs had the excellent electrical and optoelectronic property with high hole mobility 463cm2/V.sec [28]. Ga(1-x)InxSb NWs grown by the tuning of 'x' element, which did not change the Zinc blende crystal structure, nevertheless, Ga0.6In0.4Sb growth had p-type conductivity [29]. For the growth of increased hole mobility Ga0.75In0.25Sb QW structure, Al0.95Ga0.05Sb was used as buffer layers, which was grown by the molecular beam epitaxy. Ga0.75 In0.25Sb QW revealed the highest hole mobility of 1170 cm2/V.sec [30].

Fourth growth method: The crystal growth in microgravity; the shape of interface was nearly flat in μg, but the highly facets at the edge were observed in 1g. The EPD was low at faster growth rate in μg [31,34]. The In0.11Ga0.89Sb crystal grown in the space, the uniformity in the composition achieved for a higher growth rate in μg. The uniformity in composition not achieved in 1g due to the steady state equilibrium in the melt composition by convection. The non-steady state equilibrium in the melt composition was achieved in μg [32,33]. The homogeneous growth of Ga1-

xInxSb by temperature freezing method was achieved in μg but the interface shape and composition affected in 1g condition [35]. The crystal growth studied in μg, and influence of gravity on growth were analysed in zero gravity [36]. The highly immiscible alloy (HMA) Al-Bi-Sn grown in μg by directional solidification attributes the ordered microstructures, no visible gas cavity or pinhole. The convective flow of the melt and the Stokes motions of the minority phases (gas bubbles) were diminished in μg. The detached growth was promoted in μg, although, the growth controlled by thermal diffusion, hydrostatic pressure and wall effect [37]. In the alloy TC8 (Ti, Al, Mo, Si) growth in μg, and in 1g, the microstructure, the convection, and solute transport was affected by gravity and the grain sizes were smal. The solidification velocities of crystal were rapid having low influence on microstructure in μg, [38].

Fifth growth method: The thermoelectric (TE) method, the 'In' doped GaSb for the Ga(1-x)InxSb, (x=0 to 0.2) invented by combining melting with Spark Plasma Sintering (SPS) at 873 K for 15 min with the 60 MPa axial compressive pressure under vacuum. Experimentally proved that the In doping into GaSb (Ga sites), the lattice thermal conductivity reduced by replacing Ga with In, then a ZT value increased up to x=0.02, while increase of In doping beyond certain limit, decreased the power factors, and ZT values [39]. The anion vacancies increase the carrier concentration, and then suppressed bipolar effect increasing ZT [40]. The HMAs modifies the electronic band structures, which is important in developing the high TE, and the band-gap enhancement is possible. Decreasing electrical conductivity as function of anion (Sb) increase carrier concentration then increases thermoelectric power factor and ZT. The doping as function of the large thermoelectric power factor and ZT is subject of on-going research [41].

We have designed and fabricated the home made VDS-process for the III-V entirely detached the binary, ternary, and doped high-quality bulk crystals. These detached crystals reveal the self-control on the buoyancy convection and hydrostatic pressure. The element distributions in detached growth have no major change because of the composition percentage and no macroscopic segregation. Crystal's properties of entirely detached are enhanced due to decreased native/active defects and dislocations by increased crystallization. The detached phenomenon has been proved by the successful growth of three III-V bulk crystals grown using VDS-process [42-55].

The study presented in this manuscript is based on the homogeneous and entirely detached Ga(1-x)InxSb (x=0.10, 0.15, 0.25) crystals grown by the VDS-process. Distribution of 'In' doping into entire detached Ga(1-x)InxSb crystal and effect of composition % on the crystal properties have been investigated.

II. EXPERIMENTAL PROCEDURE
2.1. Preparation of growth

The pseudo-binary crystal growth is the problematic and a challenge. Despite of the growth hurdles, the efforts have been made to grow three Ga(1-x) InxSb (x= 0.10, 0.15, 0.25) ingots by VDS-process. One side tapered ampoule was cleaned by the high temperature flame prior to sealing for the III-Sb based growth. The stoichiometric source materials (Ga, In, Sb) were placed inside the cleaned ampoule for a sealing. Oxygen, nitrogen and impurity contaminations of these source materials were eliminated. An ampoule with vacuum ~1.3x10-3Pa refilled by high-purity argon gas, and purged alternately 10 times. Finally, the Ga, In, Sb source materials and a quartz ampoule sealed with backfilled high-purity argon of 20-30KPa. The vacuum sealed ampoule positioned vertically in the specially designed and fabricated vertical furnace (VDS-process) Fig-1a. A conical tip angle of an ampoule was designed to ~450 to~750, diameter 10-22mm and length ~50-75mm to grow bulk Ga(1-x)InxSb crystals.

Ga(1-x)InxSb is a pseudo binary growth of the InSb-GaSb phase having the solidus-liquidus phase temperature difference > ~1000C at x=0.5, it is a non-reactive growth region [8]. Non-controlled crystal growth was heterogeneous by effect of composition % 'x' [7]. The major complication of Ga(1-x)InxSb growth are the phase change, heat transfer, fluid flows, solute transport, and segregation, which affects crystalline growth. The basic problems are the influence of the convection, thermal stress, eutectic growth, grain and twins boundaries, segregation, micro-cracks, inclusions and the constitutional super cooling (CSC) [10,11]. To overcome the aforesaid growth complications, a vertical furnace was specifically designed and fabricated for the crystal growth of III-V Sb-based bulk crystals using VDS-process [40-53] Fig-1. The vertical furnace temperature profile is shown in Fig-1b,c, Red-L, a line of the liquidus, Green-S, a line of the solidius and Black 'x', the composition % along the growth direction, modified from the pseudo binary phase growth [8]. The ingot growth begins always below the centre of furnace, hence liquidus (L)-solidus (S) curves never meet with each other in the higher temperature gradient zone Fig-1 c. In low temperature gradient zone, the liquidus-solidus curve meets at the point 'C' (crystallization point); the L, S, and 'x' lines meet at the point 'C' to begin
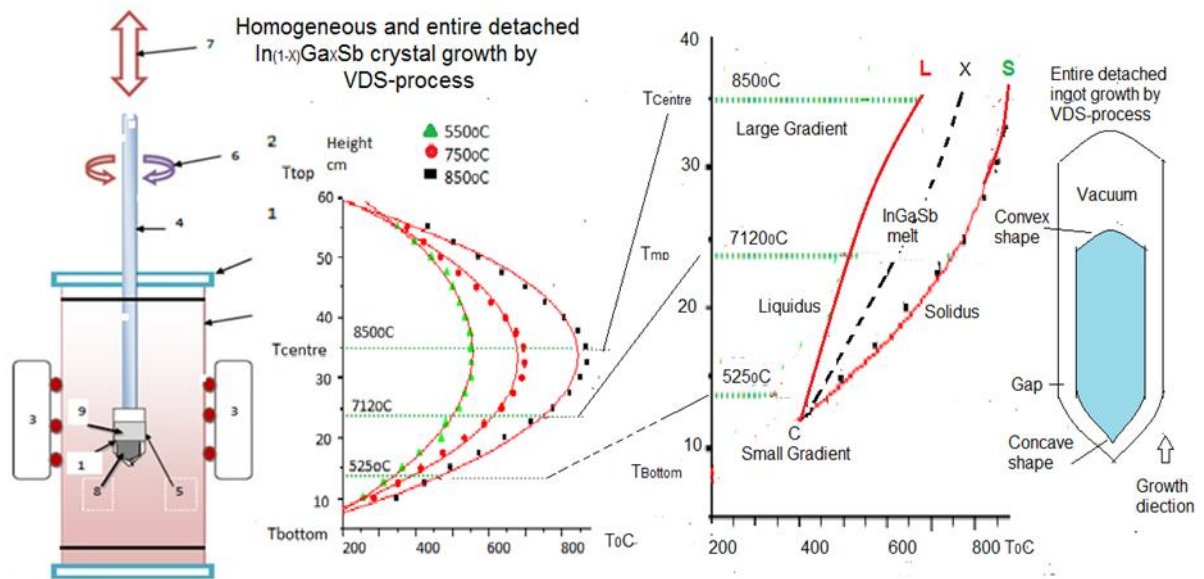
Figure- 1 The schematic diagram of the VDS process a: the numbers in 1a, the quartz growth chamber, 2) Wilson seals, 3) a vertical furnace with the thermocouples (red circles), 4) a vertical shaft to hold the ampoule at the centre of furnace, 5) a vacuum sealed quartz ampoule, 6) a clockwise and anti-clockwise rotation 7) the up and down movement of an ampoule, 8) as grown detached ingot inside ampoule, 9) the vacuum (open space) above a melt, 10) the vacuum sealed quartz ampoule with source materials inside, 11) The open quartz tube covered with silicon wool, 12) The bottom Wilson seal was removed and exposed to ambient temperature. b) The temperature profile of furnace used for melt solidification. The height of furnace 66cm, and the hot zone of furnace at the centre 33cm. Below, towards bottom side the ingot process carried out, c) In VDS-process, the radial gradients is 1.40C/cm and the axial gradient decreases towards lower temperature from large gradient condition (320C/cm) to small gradient condition (120C/cm). The red-L was the line of liquidus, green-S was the line of solidius, and black 'x' was the region of the Ga-In-Sb composition % along the growth direction. d) The schematic as grown entire detached crystal (light blue colour) with a gap between the inner ampoule wall and as grown ingot.

crystallization. The crystallization process advances in upward direction by the increasing length of grown ingot. The growth of the homogeneous and uniform composition % 'x' was exhibited by the entire detached growth resulted due to control on the phase change, heat transfer, fluid flow and solute transport. Since the axial temperature gradient reduces gradually from high to low temperature, the growth is always at low temperature gradient zone, Fig-1c. Crystallization at interface (solidification) would change from m.p. 5250C (InSb) to 7120C (GaSb) in the upward direction at fixed set temperature~7600C at the high temperature gradient. The conical tip probably reduces the defects by promoting the entire detachment. The self-grown seed, and self-stabilization of pressure difference is own process during detached growth [42-55].

2.2. The entire crystal growth
The furnace temperature profile to provide heat to the melt is shown in Fig-1a,b. The growth parameters were fixed from our previous VDS-process experiments [53-54]. The brief seven steps

crystal growth process: i) the furnace temperature was raised in 3h to ~8500C (synthesis overheating condition 150°C) to melt the In-Ga-Sb source materials in a heat zone Tcentre>Tmp> Tbottom, and maintained steady for 3h for complete-congruent melting Fig-1a,b. The vertically positioned ampoule with melt was rotated continuously with rate of 10rpm using the clock-wise and anti-clockwise mechanism for the mixing of Ga, In, Sb source materials [21]. The actual calibrated furnace temperature profile is in Fig-1b. ii) The ampoule enclosed with the congruent melt was translated downward by the lowering rate 10mm/h in 3h with the fixed set temperature ~7650C (growth overheating condition 50°C). The interface changes from the m.p. InSb to GaSb (5250C to 7120C) in a heat zone Tcentre>Tmp> Tbottom (solidification process). The enlarged furnace temperature profile is shown in Fig-1c. iii) In this state, the steady isotherm was maintained for the homogeneous and chemically uniform melt for 3h. iv) In the actual growth process of an ingot, the ampoule of the homogeneous and congruent melt was translated

downward by the freezing rate ≤5μm/s (1.38μm/s) from the large axial gradient of melt (320C/cm) towards the small axial gradient (120C/cm). The enlarged furnace profile is shown in Fig-1c, where actually crystallization / solidification begin. The radial gradient was constant at 1.40C/cm. The ingot crystallization (solidification) time was ~20h for the length 100mm of ampoule (~50-75mm ingots length). The ingot growth rate in a growth chamber is ~5mm/h (1.38μm), identical for the binary, ternary and doped (72 growths) ingots of growth [42-55]. The axial and radial temperature gradients in the growth chamber of the vertical furnace have been calibrated by the vertical and horizontal temperature profile of the furnace using thermocouples Fig-1a. The ampoule lowering growth rate was fixed to 10mm/h, which was calculated using smooth quartz ampoule thermodynamical condition and earlier growth experiments [55]. v) The grown ingot was lowered below 1000C by speed of 10mm/h in 3h for cooling of the ingot (m.p InSb), and maintained for 3h. vi) The furnace temperature was lowered to 3000C within 3h (for stabilising temperature of as grown ingot), and then switched off for a natural cooling for 2h. vii) The ingot was taken out of the furnace after 3h. Total growth period by VDS-process was 48h. The schematic of detached ingot is shown in Fig-1d. The as grown ingot was removed from the ampoule by cutting it from the end opposite to the tapered end; it came out easily by just tapping the ampoule. The GaSb and Ga(1-x)InxSb (x<0.3) crystals of dia=10-14mm, and lengths ~60-75mm are shown in Fig-2. Excessive heat conduction was prevented by hanging the ampoule to a shaft in Fig-1a, and was prevented by not having downward provision.

2.3 The substrates preparation

The preferential growth direction of the VDS grown crystal ingot was (022). The detached ingots grown by VDS were sliced in the lateral and the longitudinal directions to a thickness of ~500μm at room temperature (RT). These wafers were cleaned mechanically by grinding, lapping with powder of the carborrundum (5μm) and polished to mirror finish by alumina abrasive (0.1 and 0.03μm). Substrates of detached growth look like a mirror shining by less effort and time as compared to the substrates of attached growth. Wafers were cleaned

in warm TCE, acetone and methanol of electronic grade. The dimensions of the substrate used for the characterizations were 10x10x0.5mm3. Ohmic contacts were prepared at the four corners of substrate to measure electrical parameters by Hall-van der Pauw method.

2.4 Measurement and characterizations

The measurements were: i) The substrates cut of required dimensions by Buchler ISOMAT Low speed saw and diamond cutter using Low Speed Saw and Metacut-DC-I. ii) The substrate was prepared to the mirror finish by Metapol DC-II. iii) Growth morphology was developed by selective chemical etching CP4, and modified CP4. iv) The crystal dislocation density (dd) were measured using Metallurgical microscope (Carl Zeiss, Karl Suss MJB-3, Metagraph-I Metatake), and Interface contrast microscopy Nomarsky (Leitz Arisomet vaviport wild 46). v) The structures of samples were investigated by X-ray diffraction (JEOL JDX8030, SIEMENS Krystalloflex diffractometer) using CuKα radiation, λ=1.504Ao, Laue spectrometer (Huber) was used for the single crystal growth and orientation analysis. The microstructures were observed by scanning electron microscopy SEM (JEOL JSM-840). vi) The composition % 'x' was determined by EDAX (Analer Kevex). vii) Hall measurement were measured by Four probe CTI closed cycle Liquid helium crystal model No M22 with Keithley-220-current sources, 182-nonovoltmeter. viii) Energy gap was measured by FTIR (Perkin-Elmer-GX), Spectrum-65, Biorad-45, IR-measurement (ISS 88). ix) Microhardness was measured by Vickers test, measurements by (MVH-I Metatak) 3. Results and discussion

3.1 Features of entire detached ingots

The surface of entirely detached Ga(1-x)InxSb ingot as a whole was smooth and slightly blackish. The ingots have not displayed on the outer surface, the micro cracks, ampoule cracks, defects, and striations Fig-2,3; because, the thermal stress at interface was reduced, which diminished the growth defects [10,11]. The ingots grown by stirred method in microgravity exhibited the decreased segregation and no cracks; the detached effect by VDS-process has changed the melt convection pattern.

Table-1 For Ga(1-x)InxSb VDS experiments, the staichiometry of source materials for the growth of Ga(1-x)InxSb. The starting masses of the Ga, In and Sb are in this table.

Sr No.	Target alloys	mass Ga (gm)	mass In (gm)	mass Sb (gm)	Total mass gm $Ga_{(1-x)}InxSb$
1	$Ga_{0.8}In_{0.1}Sb$	3.383	0.606	6.592	10.58
2	$Ga_{0.85}In_{0.15}Sb$	3.61	0.66	7.01	11.27
3	$Ga_{0.75}In_{0.25}Sb$	3.901	1.647	6.985	11.63
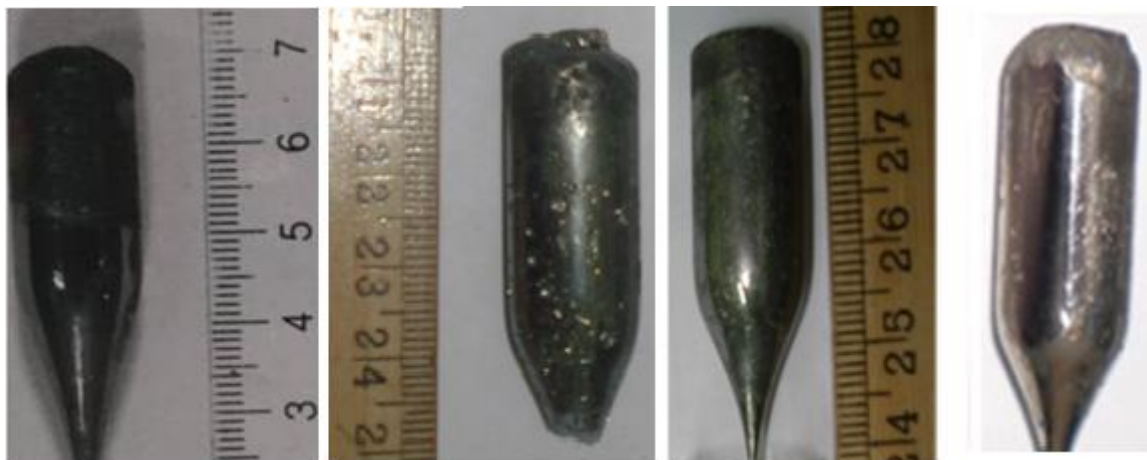
a) GaSb   b) GaInSb-1 (x=0.10)   c) GaInSb-2 (x=0.15)   d) GaInSb-3 (x=0.25)

Figure-2 The as grown ingots of Ga(1-x).InxSb, a) GaSb, b) GIS-1 (x=0.1), c) GIS-2 (x=0.15), d) GIS-3 (x=0.25). The surfaces are without growth morphology, at the beginning concave and and end growth convex are visible.

The Ga(1-x)InxSb detached ingots showed the concave shape due to melt drop shape in the beginning of growth, and the convex shape at the end of the growth might be due to surface tension effect. The smooth and shiny surface of the entire ingot growth characterises a good crystallization growth Fig-2, because, the facets growths and striations prevented in entire detached process by the reduction the native defects by passivation-compensation process [21]. But at the end of growth of the ingot, the meniscus and interface shapes are convex (seen from a vacuum), could be the effect of concentration difference. The In-Ga-Sb stoichiometric grown ingots have a convex cap at end of the growth (hemispheric), Fig-2.
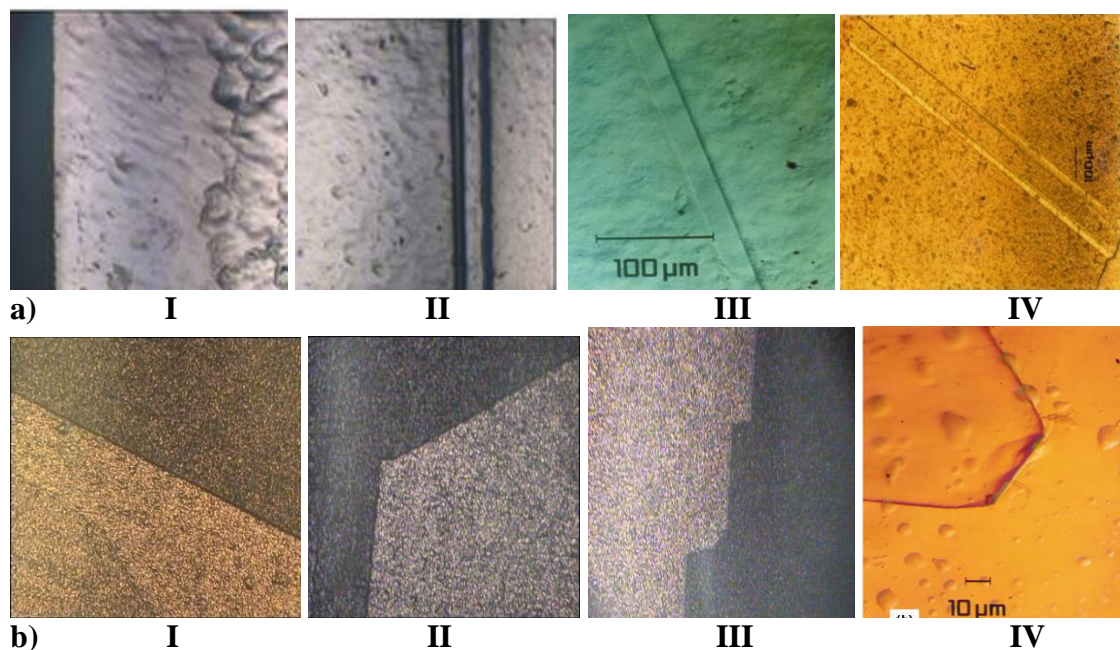
Figure-3 The growth morphology, a: I) The curve micro growth away from the edge of substrate, II) The antimony black bands at the centre of the ingot, and III, IV) The twin growth on the surface of substrate plane, b: I) A low energy plane of the twin lamellae growth, II) Energy optimization by angular faceting growth on a plane, III) Energy optimization by multi faceting growth on a plane, IV) the large grain growth on the substrate surface on another plane both plane are in different colours

The interface fluctuation into the melt is negligible, whereas, the growth destabilizing flows are confined in detached growths. Detached growth promotes a perfect crystal by the uniform thermal field and concentration distribution in stable homogeneous melt Fig-1c,d. The higher growth rate of the ingot at the solidification point 'C' results in the high-crystal quality Fig-2. It promotes a plane interface as the homogeneous melt accumulated at interface front.

3.2 Growth morphology and dislocation density

The results of the three entirely detached $Ga_{(1-x)}In_xSb$ (x=0.1,0.15, 0.25) ingots grown by VDS-process are shown. The dislocation density of the three ingots has been reduced to i) $1.42 \times 10^3 cm^{-2}$, ii) $4.39 \times 10^3 cm^{-2}$, and iii) $7.29 \times 10^3 cm^{-2}$, due to the reduced segregation, and uniform 'In' distribution. The reduced dislocation density represents the up-gradation of the crystals quality by congruent and homogenous $Ga_{(1-x)}In_xSb$ melt due to rotation (stirring) during the growth. The stirred crystals obtained a better transverse and the longitudinal distribution and transport properties Table-2,5. The indium distribution was uniform and no major fluctuations, hence, the electrical and transport properties improved contributing increase in the lattice hardness and the crystallography Table-3-5. The growth of microstructures in VDS-process depend on the experiment designing, thus the low angle (<150) twin lamellae and grain boundaries

(x=0.10, and 0.15) are shown in Fig-3. The curved microstructures away from the edge of substrate are due to the melt flows, and the thermo-capillarity concentration convection by the heat and mass transfer Fig-3aI. Thermal mechanism process was tangential through the curve of meniscus directing towards crystal-melt (C/M) interface. The black bands (Sb) of impurity at the centre of the substrate continue uniformly throughout in the vertical direction as is shown in Fig-3aII. The growth of twin lamellae shown in Fig-3aIII, IV, attributes the higher crystal quality. A coherent twin boundary is the high degree of perfection of the single crystal (binary) or the perfect crystal (ternary) growth by VDS-process. The 'In' doped first two crystals exhibit oriented single line growth of twin lamellae shown in Fig-3bI, the angular oriented growth in Fig-3II and the multi-faceted twin growths in Fig-3bIII representing the good quality ternary crystals. The growth of oriented single large grain boundary is shown Fig-3bIV. The oriented two grains were grown together as a plane mirror images at the boundary plane formed by the low angle boundaries at an angle (<150). Thus the growth of the twin lamellae is due to a single plane of atoms. The growth of coherent twin boundaries is internal structure formation by itself as indicated by the mirror image along the shared border Fig-3b. Since it is highly symmetric interface in a single crystal, the other may be its mirror image. The atoms can share the two crystals

Tabble-2 the composition % of three $Ga_{(1-x)}In_xSb$ (x<0.3) ingots measurement by EDAX

Substrate		GaInSb-1 x=0.1			GaInSb-2 x=0.15			GaInSb-3 x=0.25		
No.	L cm	Ga	In	Sb	Ga	In	Sb	Ga	In	Sb
1	1	45.22	5.91	48.87	45.87	14.28	39.85	40.07	13.68	46.15
2	1.5	43.84	6.79	49.37	45.86	14.50	39.64	39.64	14.26	46.10
3	2	43.64	7.35	49.01	45.21	14.57	40.21	39.59	14.41	46.00
4	2.5	44.53	7.22	48.21	45.8	14.11	42.09	37.46	16.10	46.44
5	3	40.59	8.46	50.37	44.61	13.48	41.91	38.56	14.84	46.56
6	3.5	40.61	7.12	51.67	46.69	10.51	42.61	38.36	15.60	46.04
7	4	37.25	10.69	52.06	45.00	11.51	43.49	38.36	15.60	46.04
8	4.5	36.46	12.03	51.51	45.83	11.01	43.16	38.03	16.35	45.62
9	5	35.52	13.86	50.62	45.33	11.87	42.83	38.03	16.35	45.62
10	5.5	39.09	10.41	50.50	45.43	11.95	42.67	37.46	16.10	46.44
11	6	41.20	9.59	49.20	45.54	12.15	42.52	36.41	15.15	46.44

at periodic intervals with low energy at the C/M interface Fig-3b. Consequently, the shape of C/M interface during growth of III-V crystal may indicate as a flat or slightly convex due to the thermal stress. The thermal stress increases with the increased dislocation density and the defects. But the twins lamellae, and oriented grain boundaries grown in the entirely detached crystals indicate reduction in the thermal stress. The dislocation density is in the range

of $10^3 cm^{-2}$ to $x10^4 cm^{-2}$ ($1.42 \times 10^3 cm^{-2}$ to 7.29x103cm-2) and the native defects have been eliminated. As a result the crystal has higher order of crystallinity which increases the lattice hardness. The perfect crystal (single mass block) is grown by the entire detached growth, which reveals diminished convective flows into the melt due to a controlled solute distribution at the interface by VDS-process [10]. Thus, the VDS-process demoted

the large thermal stress, dislocation density and defects such as the twins, micro-cracks, segregation, inclusions, and other defects [11], and the interface shape developed is nearly flat. The smaller grains and no cracks in the stirred melt as the native acceptor defects and the micro-structural growth compensates by the dopant, which in good agreement [21]. All these results are close to the results of the crystal grown in space indicate that, the detached growth by VDS-process might promote the µg condition [37]. These microstructures growth results of the entire detached Ga(1-x)InxSb (x<0.3) crystals grown by VDS-process have been compared with the detached crystal grown in space (microgravity).

The results of Vickers micro-hardness (Hv) indentations test of the three entire detached Ga(1-x)InxSb ingots are: Ga0.9In0.1Sb=3.81GPa, Ga0.85In0.15Sb= 3.73GPa, Ga0.75In0.25Sb= 3.55GPa, and the binary GaSb=4.42 GPa, where, the hardness decreases with increasing 'In' dopant. The hardness (Hv) reveals the high degree of crystalline quality and decreased dislocation density (dd) in the crystal crystallinity. The crystal structure reveals the

perfect single crystals by the extremely high order of strength, due to dd< 103cm-2 and the hardness increases by the breaking of the covalent bonds. For the perfect crystal the dd ranges from 103cm-2 to 104cm-2, and the hardness increases by the dislocation-dislocation motion. For dd >104cm-2, the hardness decreases with increase in dislocation density due to the motion of dislocation energy. The first two cases (dd) have been observed in the entirely detached crystals grown by VDS-process.

3.3 The compositional analysis

The substrates from the middle region of the three detached Ga(1-x)InxSb ingots, cut in the transverse direction to the growth axis, were selected for the compositional analysis. The percentage of composition studied by EDAX indicates that, the composition % variation significantly decreased because of the uniform distribution of elements and the homogeneous growths. Nearly uniform concentration of Ga, In, Sb elements attributed to the uniform indium distribution, and the composition % profiles in Table-2. The crystallization state arises by

Table-3 Infrared measurement of the Ga$_{(1-x)}$InxSb crystals using FTIR

Subst No.	Ga $_{(1-x)}$InxSb-1 (X=0.10)			Ga $_{(1-x)}$InxSb-2 (X=0.15)			Ga $_{(1-x)}$InxSb-3 (X=0.25)		
	W /cm	λµm	Eg eV	W /cm	λµm	Eg eV	W /cm	λµm	Eg eV
1	2531	3.951	0.313	2150	4.651	0.267	2191	4.571	0.271
3	2674	3.741	0.331	2160	4.630	0.269	2276	4.394	0.282
5	3401	2.904	0.431	2200	4.545	0.273	2300	4.348	0.285
7	4272	2.341	0.530	1851	4.503	0.275	2540	3.937	0.315
9	4675	2.140	0.579	2725	3.626	0.342	2676	3.740	0.332
11	4857	2.059	0.606	3447	2.901	0.427	2647	3.734	0.329
13	4857	2.059	0.606	3464	2.887	0.430	2678	3.735	0.332
15	4857	2.059	0.606	3527	2.835	0.481	2678	3.735	0.332

the diffusion at the axisymmetric temperature distribution due to the defects free surfaces Fig-2. The segregation coefficient of 'In', might be close to unity for the uniform composition (for k=Cs/Cl=1), hence the 'In' concentration could remain nearly uniform along the preferred (022) growth direction. It results to the high degree of crystallization of the entire detached Ga(1-x)InxSb crystal, which grow with the homogeneous composition throughout by solidification, Table-2. Nevertheless, the three ingots have identical growth parameters and conditions. The minor composition % variation established in the highly sensitive entire detached process, possibly due to vertical furnace power supply fluctuations, or minor shift at the C/M interface.

A) Ga(1-x)InxSb-1 (x=0.10) ~ L=65mm detached ingot. i) The stoichiometric Wtgms is Ga: 3.383, In: 0.606, Sb: 6.592, Table-1. ii) Actual

indium stoichiometric Wtgms is 0.606gms, thus, the indium concentration variation is 0.0093 (~0.01) mole% per mm along a growth direction. iii) Actual indium stoichiometric Wtgms of substrate-4 at 25mm is 0.2331gms. iv) From Table-2, the composition % of substrate-4 is Ga: 44.53%, In: 7.22%, Sb: 48.21%. v) The Wtgms of In 10% is 0.606gms for L=65mm, then for In% 7.22% at 25mm, its Wtgms is 0.4375gms, thus variation of In concentration for L=25mm is 0.0175mole % per mm and it is increased from 0.01mole % per mm. vi) Wtgms of In is 0.606gms for 10%, then for 0.4375gms it is 0.0722% (~0.07%). vii) In the Ga(1-x)InxSb-1-4 the composition % converted in Wtgms is Ga0.93In0.07Sb. The mobility of substrate-4, µ=1236cm²/V.sec, and resistivity ρ=3.1x10-3Ω.cm Table-5. Thus, Ga0.93In0.07Sb has p-type conductivity and highest hole mobility

1236cm^2/V.sec, than GaSb mobility 1125cm^2/V.sec [12,15,16] due to the reduced native defects of 'Ga' vacancies by 'In' doping. Nonetheless, the 'In' dopant is isoelectric for 'Ga', hence, it increases the carrier mobility of the ternary entire detached Ga(1-x)InxSb crystals due to reduction in native defect such as vacancy (V_{Ga}, $V_{Ga}V_{Sb}$, V_{Sb}) and antisites (Ga_{Sb}, Sb_{Ga}) by passivation and compensation [10,18,2021]. This is consistent with the results of detached crystal growth of Ga(1-x)InxSb crystal indicating mobility greater than the GaSb crystal [23,24,29,30]. The aforesaid the carrier concentration by passivation-compensation of the point defects, and vacancy. Further, increase in the 'In', increases the anions (Sb), that results to increase in the carrier concentration, which converted Ga0.85In0.15Sb ingot from p-type to n-type conductivity [18]. C)

procedure was repeated for the other two detached ingots, Ga(1-x)InxSb-1(x=0.15), and Ga(1-x)InxSb-1(x=0.25).

B) Ga(1-x)InxSb-1(x=0.15), L=51mm detached ingot: The composition % for the substrate-2 has Ga0.85In0.15Sb, the electron mobility μ=2481cm^2/V.sec, and resistivity ρ=1.11x10^{-3}Ω.cm. The detached ingot converts from p-type conductivity to n-type conductivity. The 'In' dopant element as an isoelectric for 'Ga' element in Ga0.85In0.15Sb detached ingot; the increase in 'In' dopant decreases the carrier mobility and increases Ga(1-x)InxSb-1(x=0.25) ~ L=73mm detached ingot. The ingot has n-type conductivity due to the excess composition % 'x'. The substrate-2 has a composition Ga0.75In0.25Sb, the electron mobility μ=5032cm^2/V.sec, and resistivity ρ=1.99x10^{-3}Ω.cm. Ingot has throughout
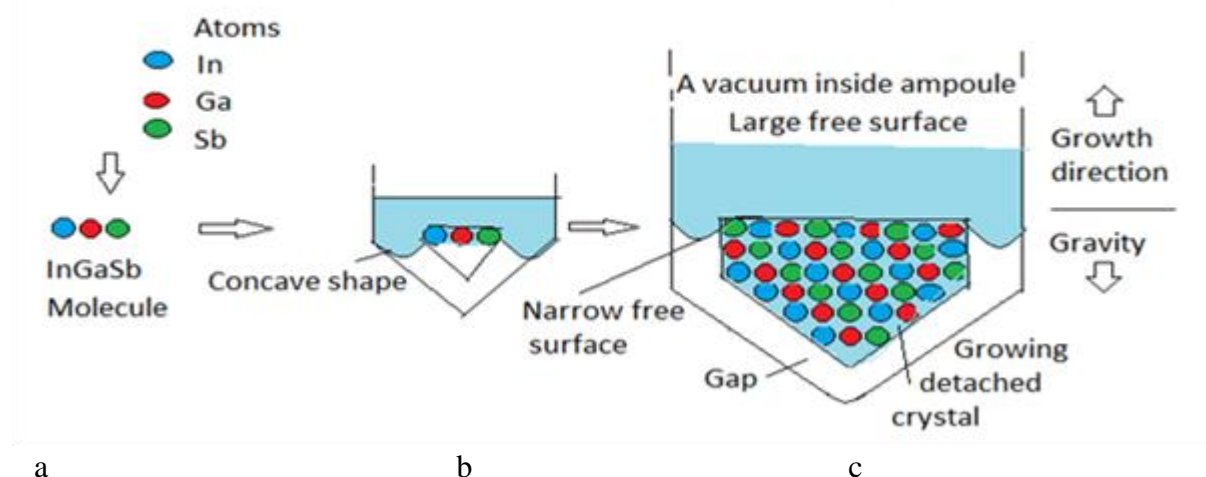

Figure-4 The schematic growth process of the Ga(1-x).InxSb crystal at the atomic level by VDS-process.
n-type nature because of excessive anions. The carrier concentration has been decreased compare to first two growth due to the increased 'In' component entrapped the electrons, Table-5. Finally, these three detached growth, we have concluded that the first two detached growth the equilibrium coefficient of composition % <0.2, while third detached growth the equi **3.4 Energy gap measurements**

The energy band gap ('Eg) of the three Ga(1-x)InxSb detached ingots was measured by FTIR at 300K for the Infrared analysis and the observations of the wave number, wavelength and energy gap are tabulated in Table-3. Results indicated the uniform stoichiometric growth, the good crystallinity, and high-quality growths with the uniform and phase-purity crystallization. The band gap engineering ranges have stated here for respective growths -- i) Ga(1-x)InxSb (x=0.10) is 0.31eV to 0.61eV, ii) Ga(1-x)InxSb (x=0.15) is 0.27eV to 0.48eV, iii) Ga(1-x)InxSb (x=0.25) is 0.27eV to 0.33eV [9-10]. These results exhibit the composition % potential for

SWIR, MIDIR [3,4,9] and Thermoelectric devices [39-411

The variations in the energy band gap (Eg) with the 'In' dopant in GaSb along growth direction are tabulated inTable-3. The energy band gap of the Ga(1-x)InxSb ingot has lower value than the energy gap of binary GaSb (Eg=0.68eV), Eg from tapered growth increases along growth direction for respective Table-3. Since the dopant 'In' acts as p-type acceptor, which occupies the shallow state above the valence band, the Fermi level shifts up by the acceptors. The transition from the new band energy level to the conduction band energy level

requires low energy, hence EObs<Eg. Effective energy state level given by Urbach tail (EU) and Burstein-Mass effect (EBM). EObs <Eg, therefore, Eg = EObs + EU - EBM. Energy shift is inversely proportional to effective mass as per the Burstein-Mass equation (BM). This confirm the high-quality Ga(1-x)InxSb entire detached growth with the tuned band gap modified by the 'In' composition % 'x', is also applicable for the recent devices [1-6].

3.5 Structural measurements

Measurements of XRD powder diffraction of the three Ga1-xInxSb ingots of the (022) growth direction are shown in Table-4. The peaks indexed to crystal planes are compared with the standard ASTM/ JCPDS GaSb No. 07-0215 and InSb card No. 07-0215. The XRD patterns of the Ga(1-x)InxSb ingots are well indexed to pristine GaSb. The 2θ peaks are slightly shifted towards low angle from the standard 2Θ=41.860A0 (binary

GaSb) as the 'In' has larger ion radius; which also confirms that the 'In' is successfully incorporated into the crystal lattice of the three Ga(1-x)InxSb crystals. The sharp peaks (x=0.10 and x=0.15) reveal that, the growths are well-crystallized, in fact, the Ga(1-x)InxSb ingots

Table-4 XRD Measurements of the GaInSb-2:

The crystal data of this table are used to compare with the standard diffraction data of the GaSb, ASTM (JCPDS) card number 7-215, for the standard diffracted angle 2Θ=41.860, lattice distance d=2.156A^0 and Miller indices h k l =022. We have used the corresponding data of this table (Italic numbers highlighted in black) for the explanation.

GaInSb 2-3		GaInSb 2-6		GaInSb 2-9		GaInSb 2-13		GaInSb 2-16	
	d	2Θ	d	2Θ	d	2Θ	d	2Θ	d
23.73	3.744	24.14	3.705	24.06	3.696	23.80	3.736	24.21	3.708
39.34	*2.230*	*39.68*	*2.227*	*39.94*	*2.255*	*39.71*	*2.227*	*39.68*	*2.225*
46.54	1.956	46.87	1.936	47.40	1.916	46.88	1.936	46.86	1.933
57.12	*1.62*	*57.13*	*1.64*	*58.14*	*1.585*	*57.22*	*1.609*	*57.15*	*1.67*
62.89	1.474	62.86	1.478	62.11	1.474	63.00	1.474	62.82	1.471
71.35	1.323	62.86	1.478	73.26	1.291	63.14	1.476	63.05	1.478
71.64	1.319	71.75	1.315	78.56	1.217	71.98	1.311	71.69	1.317
76.42	1.243	76.92	1.238	76.93	1.155	76.90	1.239	76.94	1.239

indicates the zinc blend crystal structure of the original binary GaSb crystal [18]. The solubility of In is <0.2. However, the observation of shoulders of diffraction peaks indicate the minor secondary phase in the x=0.25, which proves that, in the detached growth empowered homogeneity of 'In' dopant in GaSb. Further it is confirmed that the 'In' doping introduce lattice distortion resulting in the broadening of XRD peak as a function 'x' component >0.2. The full width at half maximum (FWHM) has been increased from GaSb 97arcsec to 124, 145 and 193arcsec for respective growths. The XRD analysis of the lower angle diffraction attributed to increased 'd' and decreased FWHM which reveals an expansion of cells by 'In' doping in Ga(1-x)InxSb. Width of the diffraction peak decreased with the increased peak intensity in response to the decrease in the dislocations density, segregation and defects; establishing higher crystallinity associated with the phase transformation and orientation of the atoms. FWHM of (220) peak of the primary phase is increasing with increasing 'In', it is confirmed into GaSb pristine affording a larger phase space by suppressing κL and improving ZT [39]. Three Ga(1-x)InxSb ingots

indicated increase in the crystallinity by reducing native vacancy and antisites in the GaSb crystal. The lattice constant of Ga(1-x)InxSb and energy gap modified by 'In' element as an isoelectric dopant for Ga, is also reported in [18,20]. librium coefficient of composition % >0.2, consistent with [7].

3.6 Electric measurement

For the electric measurements, the substrates from the middle part of the Ga(1-x)InxSb ingots were selected. The Hall–van dcr Pauw measurements of the entire detached Ga0.9In0.1Sb growth presented the highest hole mobility ~1236cm2/V.sec indicating the suppression the point defects, vacancy, antisite, and the p-type conductivity is investigated [23,24,30]. The In0.85Ga0.15Sb ingot converts from the p-type conductivity (charge carriers holes) to n-type conductivity (charge carriers electrons) due to increase in the anions concentration [18, 21]. We have investigated that the very small transient region between the p-type to n-type has the flip-flop state, this unstable state of the carriers force itself to reach the stable state of carrier. In the Ga(1-x)InxSb (x<0.3) detached growths, 'In' doping

Table-5 The measurement by the Hall-van der Pauw effect at the 300K of the three $Ga_{(1-x)}InxSb$ (x= 0.10, 0.15, 0.25) ingots grown by VDS-process

Growth no-1 $Ga_{(1-x)}InxSb$, x=0.10

Growth In =0.1%	GaInSb-1-02	GaInSb-1-04	GaInSb-1-07	GaInSb-1-10
Mobility (cm2 / V.sec)	518	1236	782	637
Resistivity (Ohm-cm)	3.10×10^{-3}	3.39×10^{-3}	4.42×10^{-3}	5.5×10^{-3}
Carrier Con (cm-3)	2.86×10^{18}	1.50×10^{18}	1.67×10^{18}	1.78×10^{18}
Hall Coeff cm3/ Coul	+1.62	+4.86	+3.46	+3.51

Growth no-2, $Ga_{(1-x)}InxSb$, x=0.15

Growth In=0.15%	GaInSb-2-03	GaInSb-2-06	GaInSb-2-12	GaInSb-2-9
Mobility (cm^2/ V.sec)	2481	2378	1527	1083
Resistivity (Ohm-cm)	1.11×10^{-3}	6.7×10^{-4}	4.18×10^{-4}	2.18×10^{-3}
Carrier Con (cm^{-3})	2.25×10^{18}	4.26×10^{18}	1.81×10^{18}	6.81×10^{17}
Hall Coeff cm^3/ Coulo	-2.78	-1.47	-3.7	+0.51

Growth no. 3 $Ga_{(1-x)}InxSb$, x=0.25

Growth In=0.25%	GaInSb-3-01	GaInSb-3-4	GaInSb-3-7	GaInSb-3-11
Mobility (cm^2/ V.sec)	5032	4635	3159	2147
Resistivity (Ohm-cm)	1.99×10^{-3}	1.9×10^{-3}	2.39×10^{-3}	1.9×10^{-3}
Carrier Con (cm^{-3})	3.90×10^{17}	5.86×10^{17}	7.86×10^{17}	8.86×10^{17}
Hall Coeff cm^3/ Coulo	-2.02	-1.91	-1.32	-1.13

Simultaneously reduced the lattice thermal conductivity with increasing the hole carrier mobility, and increased the carrier concentration (x=0.10 and 0.15) from 1017 to 1018cm−3, one orders of magnitude higher than that of the pristine GaSb (2×1017cm−3), due to more valence electron up to x<0.2. This is one order higher than that (2×1017cm−3) of the pristine GaSb. The excess anionic vacancies by 'In' doping found that increased the carrier concentration and

transport properties of Ga(1-x)InxSb crystals [25]. The Ga(1-x)InxSb detached crystals showed the excellent transport and optoelectronic properties. The temperature dependent electrical measurements of Ga(1-x)InxSb-2-4(x=0.15), displayed the electron mobility 2507cm2/V.sec and 4037cm2/V.sec at 300K and 77K respectively, Table-6. The increased mobility with decreased temperature attributes to the control on the different scattering mechanisms of the defects(impurity, and dislocations

suppresses the bipolar effect. However, for x=0.25 the electron carrier concentration found at the optimum value, and the ingot was grown completely with n-type conductivity, same as the binary GaSb; possibly due to the compensation effect of cationic vacancies. This results to nearly unchanged carrier concentration Table-5. The Ga0.75In0.25Sb ingot exhibit n-type conductivity with highest electron mobility ~5032cm2/V.sec, it reveals probably homogeneous crystal growth. The increased mobility and the decreased resistivity signify that, there is good crystallization by detachment; the diverse scattering and other defects (lattice vibration,

impurity, and dislocation density) have been suppressed in the detached ingots. The mobility of three entire detached crystals highest than binary Table-5 is also reported in [18,23,24,29,30]. The increase in mobility is due to preference to 'Ga' sites and valence site is close to the atomic radius. It established that the 'In' doped GaSb crystal has uniform C/M interface shape by decreased 'Ga' native defect and segregation which increased the).

3.7   Thermoelectric (TE)   Characterization
Thermoelectric (TE) effect is a process which directly converts heat energy into electricity, hence the TE materials has potential applications in power generation. Thermoelectric figure-of merit (ZT) is the conversion efficiency as the ZT =S2σT/κ [39], where, S: Seebeck coefficient, σ: electrical conductivity, κ: total thermal conductivity, and T: absolute temperature. The thermal conductivity κ is an electronic and a lattice component, then κ= κE +κL. The doped GaSb crystal has increased TE property by increased electrical transport properties. The 'In' doping in GaSb reduces thermal conductivity. The 'In' as isoelectronic substitution for 'Ga' could acts as scatter of phonons and reduces the lattice thermal conductivity. Experimental results of the 'In' doped into GaSb reported that the lattice thermal conductivity reduces, and then ZT value increases. The thermoelectric (TE) properties enhanced by the Ga(1-x)InxSb (x<0.2) crystalline materials due to the presence of the point defects and composition segregations. The doping defects acts as phonon scattering centres that contribute to the weak

influence on electrical transport and reduce the | lattice thermal conductivity (κL).

Table-6 The low temperature measurement of the $Ga_{(1-x)}InxSb$-2-4(x=0.15)
detached crystal growth .

GaInSb 2-4 Temp(K)	Mobility cm^2/V.sec	Resistivity Ohm-cm	Carrier Con cm^{-3}	Hall Coeff cm^3/ Coulo
300	2507	1.64×10^{-3}	1.52×10^{18}	4.21
270	2436	1.61×10^{-3}	1.59×10^{18}	3.92
230	3082	1.20×10^{-3}	1.69×10^{18}	3.69
168	3603	9.29×10^{-4}	1.87×10^{18}	334.71
100	3994	7.53×10^{-4}	2.08×10^{18}	300.75
77	4037	7.22×10^{-4}	2.14×10^{18}	291.47
60	4053	7.00×10^{-4}	2.20×10^{18}	283.71
40	4039	6.91×10^{-4}	2.24×10^{18}	279.09
30	3994	6.87×10^{-4}	2.28×10^{18}	274.39
20	3964	6.85×10^{-4}	2.30×10^{18}	271.53

The lattice vibration control, structural imperfections and defects engineering (point defects, segregations) show effect on electron and phonon transport properties and reduce lattice thermal conductivity [39]. The decrease in the electrical conductivity as a function of dopant results in large values of thermoelectric power factor (Sσ) and ZT [40], the subject of on-going research [41]. Detached III-V crystal growth by VDS-process has optimum high mobility, increased the carrier concentration (reduced the bipolar effect), and the reduced resistivity. The reduced thermal conductivity increases the thermoelectric power factor and figure of merit ZT. The research of the detached crystals for TE materials is under process**.**

3.8 The principle of entire detached growth by VDS-process
Detached growth by VDS-process, the perception is schematically expressed in Fig-4, details in [53,54]. We are summarizing the perception of the detached growth basis of the experimental results. The source materials Indium (In), Gallium (Ga) and Antimonide (Sb) at atoms level in solid circles (colors) – 'In' in blue, 'Ga' in red, 'Sb' in green, and the 'GaInSb' molecule is shown in Fig-4a. The strong bond of the In-Ga-Sb atoms arises, then the molecule appearances under the optimum growth Fig-4b. Spontaneously a tiny melt drop of homogeneous melt emerges in 3-D structure by binding energy of In-Ga-Sb atoms Fig-4c. The entire dangling melt drop detaches into tapered end of an ampoule by the influence of the binding and bonding energy of the molecules. The drop develops away from the inner wall of an ampoule (dangling melt drop). It designates self-crystalline growth away from the inner wall of an ampoule. This progression set in motion serendipitously as the apparition of a gap. Further,

the melt drop forms solid by solidification (crystallize) by slow freezing, hence, it propagates the solidification or crystallization process Fig-4. It spontaneously promotes the concave meniscus and concave C/M interface. The concave solidified tip (solid or seed) of the ingot is shown in Fig-4c. The schematic shape and the true shape are shown in Fig-1d and Fig-2 respectively. The chemically uniform structure and the homogeneous melt freezes, i.e. the uniform mass single block (perfect single crystal) grow. Thus, the self-selected spontaneous preferential growth starts with (022) direction of the crystalline structure. The seed grows under the significantly decreased buoyant and thermo-gravitational convection, the optimum surface tension and Marangoni effects into the melt (possibly as μg condition) [31-38]. The length of entire detached crystal increases continuously in vertical direction with the time, schematically shown in Fig-1d. The melt forms a concave meniscus shape with the inner wall of the ampoule along the growing crystal, i.e. blue curve shape. The concave meniscus and concave crystal-melt interface could be developed by the melt free surface area. The initial thermal conductivity has a large aspect ratio, A=H/L (melt height/crystal length), thus the meniscus and the crystal-melt interface concavity at the beginning is higher. As the crystal length increases, thermal conductivity of the crystal increases, which decreases aspect ratio, and hence, interface concavity decreases. This leads to envisage that the meniscus shape and the C/M interface shape gets converted from the concave to plane and plane to convex along the growth direction due to the contactless Ga(1-x)InxSb crystal. This is confirmed by the actually observed convex shape of the upper end at the every crystal growth by VDS process. We contemplate that the self-seed growth and the self-stabilization of the gas pressure is the challenging

process in the entire detached growth was achieved [16]. The formation of non-steady growth can be controlled by the optimum surface tension effect and the Marangoni effect.

IV. CONCLUSION

The bulk growth of three Ga(1-x)InxSb crystals with entire detachment of the crystals was successfully carried out first time, by the novel VDS-process. The composition of 'In' doped crystal's reveals the uniform structure with the 'In' segregation significantly reduced along radial and axial direction. The dislocation density of three ingots reduced to i) $1.42 \times 10^3 cm^{-2}$, ii) $4.39 \times 10^3 cm^{-2}$, and iii) $7.29 \times 10^3 cm^{-2}$. Hall mobility of the carriers in Ga0.9In0.1Sb, Ga0.85In0.15Sb, Ga0.75In0.25Sb enhanced to $1236 cm^2/V \cdot s$ (p-type), $1083 cm^2/V \cdot sec$ (p-type to n-type conversion), $5032 cm^2/V \cdot s$ (n-type) respectively. The results confirmed that the carrier mobility of doped Ga0.9In0.1Sb is higher than the binary GaSb crystals. The axial resistivity reduced to $10^{-3} \Omega \cdot cm$. The reduced dislocation density, low resistivity and the highest mobility postulate the crystalline and stoichiometric growth of the ternary Ga(1-x)InxSb crystals. The uniform phase purity specifies the crystalline quality and the preferred (022) growth direction. The compositional analysis and characterization of entire detached Ga(1-x)InxSb crystals grown by VDS-process, reveals the higher growth velocity, reduction in the buoyancy convection and solute transport effects. The detached growth promotes the crystallization and solidification by preventing the microstructure and self-control on the hydrostatic pressure and thermal stress. Thus the detached growth is an effective process which introduces diffusion at atomic level. Thus the detached growth is an effective process which introduces diffusion at atomic level. We have verified the elimination of the boundary, eutectic growth, growth morphology and segregation in entire detached growth. The compositional uniformity is achieved by higher growth rate. The crystal growth in space showed that the buoyancy convection, hydrostatic pressure, sedimentation disappear, and the crystal quality improved dramatically. The stability and surface features of the entire detached ingots grown by VDS-process are close to the detached crystal growth in space. The uniformity, smooth surface, reproducibility, and repetition signify the "detached phenomenon" as well the crystalline high-quality properties of the entire detached Ga(1-x)InxSb crystal.

REFERENCES

[1]. Del Alamo, J. A. Nature 479, (2011).317
[2]. LaPierre R., Robson M., Azizur-Rahman K, Kuyanov P; J. Phys. D: Appl. Phys. 50, (2017).123001
[3]. Ma, Z Qin, G Xie, L Qian, D Tang Appl. Phys. Rev. 6, (2019) 021317
[4]. R. Peng, S. Jiao, H. Li, L. Zhao,J. Alloy.omp. 632 (2015) 575–579.
[5]. Li, Z. Nanotechnology. 26, 445202 (2015).
[6]. S. Abroug, F. Saadallah, N. Yacoubi, S. Abroug, J. Alloy. Comp. 484 (2009) 772
[7]. Krishan P B, Barman, G.S. Mudahar, N.P. Singh, Mater. Lett. 58 (2004) 1441–1445
[8]. G.N. Kozhemyakin, J. Cryst. Growth 220 (2000) 39-45.
[9]. G.B. Stringfellow, J. Phys. Chem. Solids 33 (1972) 665
[10]. J. Vincent, E. Dieguez, J. Cryst. Growth 295 (2006) 108–113.
[11]. A. Tanaka, J. Shintani, M. Kimura, T. sukegawa, J. Cryst. Growth 209 (2000) 625–629.
[12]. T. Du!ar, P. Dusserre, F. Picca, S. Lacroix, N. Giacometti J Crystal Growth 211 (2000) 434}440
[13]. Ebnalwaled, A.A. Duffar, Tb, Sylla, L. Crystal Research and Technology 48(4), (2013), 236-244
[14]. P. Boiton, N. Giacometti, T. Duffar, J. Santailler, P. Dusserre, J.P. Nabot, J. Cryst. Growth 206 (1999) 159–165.
[15]. C. Barat, T. Duffar, P. Dussere, J.P. Garandet, Cryst. Res. Technol. 34 (2015) 449–456
[16]. Lamine Sylla a, Thierry Duffar b,nJournal of Crystal Growth 324 (2011) 53–62
[17]. Wang, J, Wang, L., Teng, D., Zhai, S., Liu, J. Crystal Rese Techno 52(9) (2017), 1700092
[18]. N. Murakami, T. Hikida, A. Konno, K. Arafune, T. Koyama, Y. Momose, T. Ozawa, M. Miyazawa, M. Kumagawa, Y
[19] Hayakawa, J. Cryst. Growth 310 (2008) 1433 [19] B.C.Houchens, P. Becla, S.E. Tritchler, A.J. Goza, D.F. Bliss, J. Cryst. Growth 312 (2010) 1090–1094
[20]. R- M. Streicher, V. Corregidor, N. Catarino, L.C. Alves, N. Franco, M. Fonseca, L. Martins, E. Alves, E.M. Costa, Nucl. Instrum. Methods B. 371 (2016) 278–282
[21]. Cândida Cristina Klein, Berenice Anina Dedavid, Kendra D' Abreu Neto Fernandes, Nestor Cezar Heck, Int. Eng. J., Ouro Preto, 69(4), (2016) 465-471 . |
[22]. Jianbin Wang, Liya L. Regel, William R. Wilcox Journal of Crystal Growth 260 (2004) 590–599
[23]. Q Liu, J Wang, G He, D Yang, W Zhang, J Liu; Vacuum 174 (2020) 109177

[24]. Wang R, Wang I He G, Yang D, Zhang D, Liu I J Mater Sci Maters Electronics 30(16) (2019) 15654-15661

[25]. O.Paatzold, K. Niemietz, R. Lantzsch, V. Galindo, I. Grants, M. Bellmann, G. Gerbeth Eup Phys J-Spec Top 220 (2013) 243–257

[26]. A. Mitrica, T. Duffara, C. Diaz-Guerrab, V. Corregidorc, L.C. Alvesc, C. Garniera, G. Viana, J. Cryst. Growth 287 (2006) 224–229

[27]. Li, X., Zhang, Z., He, Gb, Yang, Dc, Zhang, Wc, Liu, J Japanese J Appli Phys 59(5) (2020) 055503

[28]. Dapan Li, Changyong L, Arumugam M,SenPo Y, Ziyao Z, Xiaoguang L, Lei S, Yu-Lun C, Ning H, Johnny C; Nature Communications, 10 (2019) 1664 1234567890

[29]. Gorji Ghalamestani, S, Ek, M, Ganjipour, B, Thelander, C, Johansson, J, Caroff, P. Dick, K.A,bNano Letters Volume 12, Issue 9, 12 September 2012, Pages 4914-4919

[30]. Roh, I.b, Kim, S., Geum, D.-M., Lu, W., Song, Y., Del Alamo, J.A., Song, J.Applied Physics Letters 113(9} (2018) 093501

[31]. Y Inatomi, K Sakata, M Arivanandhan, G Rajesh, V Nirmal Kumar, T Koyama, Y Momose, T Ozawa, Y Okano, Y Hayakawa, npj Microgravity 1 (2015) 15011

[32]. J Yu, Y, V N Kumar, Y Hayakawa, Yi Okano, M Arivanandhan, Y Momose, X Pan, Y Liu, X Zhang, X Luo, npj Microgravity 5 (2019) 8

[33]. Jianding Yu, Yuko Inatomi, Velu Nirmal Kumar, Y Hayakawa5, Y Okano, M Arivanandhan, Y Momose5, X Pan1, Y Liu1, X Zhang X Lu, npj Microgravity 5 (2019):8

[34]. Y Inatomi, K Sakata, M Arivanandhan, G Rajesh, V Nirmal Kumar, T Koyama, Y omose, T Ozawa, Y Okano, Y Hayakawa, npj Microgravity, 1 (2015) 15011

[35]. Yu, J. Liu, Y, Pan, X, Zhao, H, Kumar, V.N, Arivanandhan, M., Momose, Y, Hayakawa, Y, Zhang, X, Luo, X, Okano, Y, Inatomi, Y. Microg Sci Techno 28(2) (2016) 143-154

[36]. V. I. Strelov, I. P. Kuranova, B. G. Zakharov, E. Voloshin Crystallography Reports, 59(6) 2014, 781–806.

[37]. Hongxiang Jiang, Shixin Li1, Lili Zhang, Jie He, Jiuzhou Zhao, npj Microgravity 5 (2019) 26

[38]. Xinghong Luo, Yaya Wang, Yang Li npj Microgravity (2019) 5:2

[39]. Shan Yun, Tan Guo, Yanxing Li, Jiadong Zhang, Huaju Lia, Jing Chen, Litao Kang, Aibin Huangb, Ceramics International 44 (2018) 22023–22026

[40]. Zhengliang Dua, Jian Heb, Xiaolu Chena, Mengyi Yana, Junhao Zhuc, Yamei Liub Intermetallics 112 (2019) 106528

[41]. S. AlFaify, 1, Bakhtiar Ul Haq, 1, R. Ahmed, Faheem K. Butt, M.M. Alsardia Journal of Alloys and Compounds 739 (2018) 380e387

[42]. Gadkari D.B., J Chemi Chemi Enginee 6,2012 65,

[43]. Gadkari D.B., J Chemi Chemi Enginee 6,2012 250

[44]. Gadkari Dattatray, J Materi Sci Engin A3 2(9),2012, 593

[45]. Gadkari D.B., Ameri Insti Phys, Conf Pro 1512,2013 856

[46]. Gadkari D.B., J Materi Sci Engineeg A3(5), (2013),338

[47]. D.B. Gadkari, B.M. Arora, Material Chemistry and Physics 139 (2013) 375

[48]. D.B.Gadkari, Interna J. Sci Res Publ 4 (2014) 1

[49]. Dattatray Gadkari, Intern J Enginee Appl Sci (IJEAS) 2(4) (2015) 39

[50]. D. Gadkari, D. Maske, M. Deshpande, B Arora,Inten. J. Innov. Resea Sci. Eng 5(2)

[51]. (2016) 2092

[52]. Dattatray Gadkari, J Electro Commu Engineering (IOSR-JECE) 12(4) IV (2017), 51-58

[53]. Dattatray Gadkari, J Electro Commu Engineering (IOSR-JECE) 13(3) (2018), 21-31

[54]. Dattatray Gadkari, Int J Eng Res App 8(4) (2019) 01-19

[55]. D B Gadkari, Int J Eng Res App10(5) (2020) 7-20

[56]. D Maske, M Deshpande, D Gadkari, J Nno and Electronis Physics12 (2) (2020)2012

Dr D B Gadkari, received B Sc (Physics) degree (1974) from Shivaji University, Kolhapur and M.Sc. degree in Physics from Bombay University (1976), and then University of Mumbai confirmed M Phil (1986) and Ph. D. under UGC-FIP (1998). He joined Mithibai College, Mumbai India (Nov-1976) as a Asst Prof, then HOD- Physics (2000-14), Asso prof (2006-2014), Vice-Principal (2010-2013) and Principal-I/C (2013-2014). He was Adjunct Research Guide-Faculty of Science:

University of Mumbai (2014-2017), was at University of Mumbai- Board of Study Member in Physics (2005-2014), Faculty of Science Member (2005-2014); Board of Study Member in Bio-Physics (2010-2014). From June 1, 2017, Dr Gadkari is Freelance research and Consultant: Crystal Growth and Crystal Technology (Crystal Growth, Material Science, Solid State Physics and Physics of devices). He has been published 52 articles in referred journals and in the 32proceedings. The single crystal growth a new growth process - vertical directional solidification (VDS) has been developed successfully, and which shows the detached phenomenon concept for Sb-based (III-V) quality bulk crystals in a terrestrial lab (on Earth). These crystals showed highest physical properties for crystals grown ever, while crystals are analogous to the crystal grown in microgravity. Gadkari is Member of professional International and National research journals. He has successfully completed Research projects (nine) sponsored by government of India and parent institute (SVKM). Indian patents in his name for the detached crystal growth by VDS in the terrestrial lab. This approach has opened a new area for high quality entire detached single crystal growth. He has received several kinds of awards/medals/certificates from academic societies such as Materials Chemistry and Physics, Indian Association of Crystal Growth, ASM International India Chapter, Shivaji University Kolhapur India, Several Research Institutes / Colleges within India and also from abroad.

D. B. Gadkari. "Investigation of influence of the indium doping on the properties of the Ga(1-X)InXSb (x=0.10, 0.15, 0.25) crystals: the detached growth by the VDS-process ." *International Journal of Engineering Research and Applications (IJERA)*, vol.10 (09), 2020, pp 05-19.